NAG 1-02015

Piezohydraulic Pump Development

Final Report

Christopher S. Lynch
The GWW School of Mechanical Engineering
The Georgia Institute of Technology
Atlanta, GA 30332-0405

1. Overview

Reciprocating piston piezohydraulic pumps were developed originally under the Smart Wing Phase II program (Lynch) and later under the CHAP program (CSA, Kinetic Ceramics). These pumps focused on 10 cm scale stack actuators operating below resonance and, more recently, at resonance. A survey of commercially available linear actuators indicates that obtaining power density and specific power greater than electromagnetic linear actuators requires driving the stacks at frequencies greater than 1 KHz at high fields. In the case of 10 cm scale actuators the power supply signal conditioning becomes large and heavy and the soft PZT stack actuators generate a lot of heat due to internal losses. Reciprocation frequencies can be increased and material losses significantly decreased through use of millimeter scale single crystal stack actuators.

We are presently targeting the design of pumps that utilize stacks at the 1-10 mm length scale and run at reciprocating frequencies of 20kHz or greater. This offers significant advantages over current approaches including eliminating audible noise and significantly increasing the power density and specific power of the system (including electronics). The pump currently under development will comprise an LC resonant drive of a resonant crystal and head mass operating against a resonant fluid column. Each of these resonant systems are high Q and together should produce a single high Q second order system.

The characteristics of single crystals are critical to development of this system. The low elastic modulus decreases the resonant frequency of the small crystals relative to similar sized PZT elements. The large piezoelectric coefficients give significant fluid motion from smaller stack actuators. The low loss tangent of the crystals gives the high Q electro-mechanical resonance. As the scale is made smaller, the piezoelectric actuators can be run at increasingly higher frequency without the penalty of very large and heavy power supplies and significant heat generation, but at smaller length scales fluid viscosity restricts flow and designing check valves that operate at these frequencies is still a significant challenge. At the 10 cm length scale viscous effects are less of an issue, but the crystals become prohibitively expensive and the power source becomes very large. The 1-10 mm scale is ideal for the dual resonant system. We have sufficient confidence in the viability of the system currently under development that further development and commercialization were proposed by Georgia Tech and NextGen Aeronautics under a DARPA sponsored SBIR solicitation.

Small, highly efficient, and light weight actuators are an enabling technology for a number of aerospace applications including morphing aircraft and rotorcraft. Morphing aircraft will benefit from small light weight high power density distributed actuators. Rotocraft will benefit from actuators that can be embedded within the blade and drive trailing edge flaps at frequencies of four cycles per revolution or better.

Several technological challenges have been encountered with the 10 CM length scale pumps. The piezoelectric must deliver the maximum possible strain. This leads to selection of donor doped (soft) PZT stacks driven by unipolar voltage at 2 to 3 times the coervive field. The pumps must operate at frequencies greater than 1 KHz to obtain energy densities significantly higher than conventional electromagnetic linear actuators. Driving soft PZT at these frequencies and drive levels generates a lot of heat in the stack actuator that must be dissipated. This poses design challenges to remove the heat such as fluid based cooling or requires running a low duty cycle (pump spends most of its time off so that it can cool). To date, none of the pumps have achieved >1 KHz operation, although all are showing promise. The large PZT stacks require high voltage and high power. This results in heavy bulky power supplies and thus overall lower specific power from the system. These limitations have led to this effort to develop single crystal based pumps based on multiple resonant systems.

The resonant piezohydraulic pumping system at the smaller length scale will utilize a combination of several high Q resonant systems to produce a single high Q system. The resonant sub-systems consist of an LC oscillator for the drive element, an electro-mechanical stack / head mass resonator, and fluid resonant tube. Several properties of the single crystals are critical to successful development of such a system. These include the large piezoelectric coefficients (provides large displacement), the low young's modulus (decreases the resonant frequency for the small stacks), the high coupling coefficient, and the low loss tangent (provides high Q). This combination of properties should enable the design of a high Q resonant system operating at >20 KHz with millimeter scale stack dimensions and a fluid resonant tube on the 20 to 80 mm length scale driven by a simple LC oscillator. The overall output power of the proposed system will be 5 to 25 W.

1.1 Details of the Pumping System

1.1.1 Piezohydraulic pump background

The conventional piezohydraulic pump cycle is shown schematically in Figure 1. The piezoelectric stack oscillates a piston within a cylinder. As the piston retracts, fluid is drawn into the cylinder. As the piston extends, fluid is forced out at higher pressure.

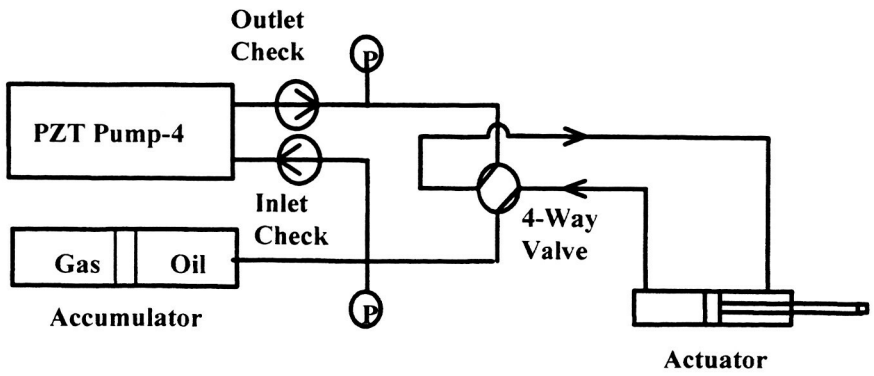

Figure 1. Schematic of the conventional piezohydraulic pump system

The thermodynamic cycle is described with reference to Figure 2.

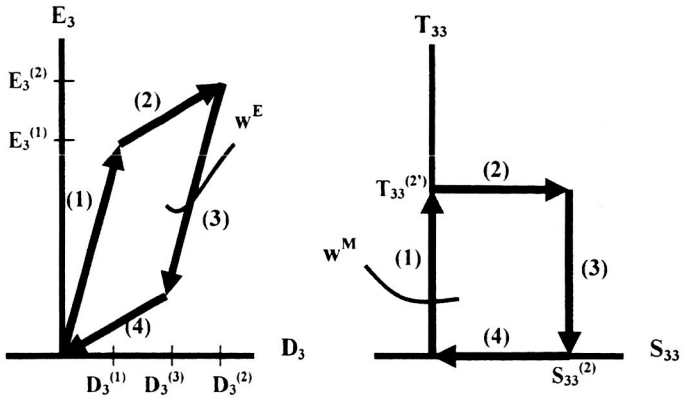

Figure 2. Piezohydraulic Pump Cycle. The area enclosed by the parallelogram in the electric field-electric displacement curve represents the electric work per unit volume required to drive the PZT stack through one pumping cycle. The area enclosed in the stress-strain curve represents the mechanical work per unit volume achieved during one pumping cycle. The efficiency of the cycle is the ratio of these areas.

The appeal of this electro-mechanical energy conversion system is that the theoretical efficiency is unity. This is shown as follows: The mechanical work per cycle is given by

$$w^M = -\left(E_3^{(2)} d_{333} T_{33}^{(2)} + s_{3333}^E T_{33}^{(2)} T_{33}^{(2)}\right) \tag{1}$$

where E is electric field, d is the piezoelectric coefficient, s is mechanical compliance, and T is stress. This is the area enclosed in the stress strain curve in Figure 2.

The electrical work density used to drive each cycle is given by

$$w^E = \frac{1}{2}\left(E_3^{(1)} D_3^{(2)} - E_3^{(2)} D_3^{(1)} + E_3^{(2)} D_3^{(3)} - E_3^{(3)} D_3^{(2)}\right) \tag{2}$$

where D is the electric displacement. The electrical work is the area within the parallelogram in the electric field – electric displacement diagram. Through use of the piezoelectric constitutive laws, the electrical work density can be expressed by as

$$w^E = -\left(E_3^{(2)} d_{333} T_{33}^{(2)} + s_{3333}^E T_{33}^{(2)} T_{33}^{(2)}\right) \tag{3}$$

The equivalence of the electrical and mechanical work yields an efficiency of 1.0. This is reduced by stack losses, electrical losses, mechanical losses, and fluid losses. None the less, this theoretical efficiency offers significant promise once piezohydraulics are fully developed.

The potential of piezohydraulics to substantially surpass the energy density and specific energy of linear electro-magnetic and conventional hydraulic actuators is apparent in Figures 3 and 4. Figure 3 shows that a wide range of currently available linear actuation systems run at or below 100 W/Kg. In all cases shown this is a complete actuation system that takes electrical input power and delivers mechanical output power. Figure 4 shows the output power density of a series of actuators. The capability of a bare stack actuator of PZT at 1 KHz and of a PZN-PT single crystal stack at 20 KHz are shown for comparison (in this case the pump cycle described above was used to determine the maximum work). A few caveats must be mentioned in conjunction with Figures 3 and 4. The output power of most commercial actuators is not specified, so 50% efficiency was assumed. The mass of power supplies for piezo pumps has not been optimized, so a mass of 1.5 Kg was assumed. This may be an overly optimistic number. In Figure 4, the output power density of stack actuators assumes impedance matching a load using the pump cycle. This provides an ideal output. Actual output will be lower due to frictional, material, and viscous losses. The point of putting this data on the plot is to demonstrate the ideal from which the design process begins.

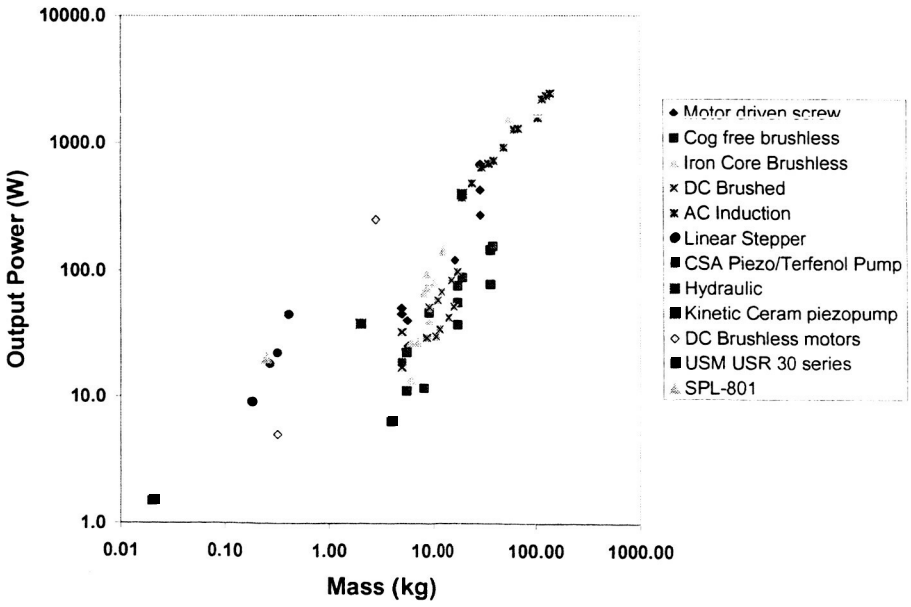

Figure 3. Output power vs. mass for a range of available linear actuation systems.

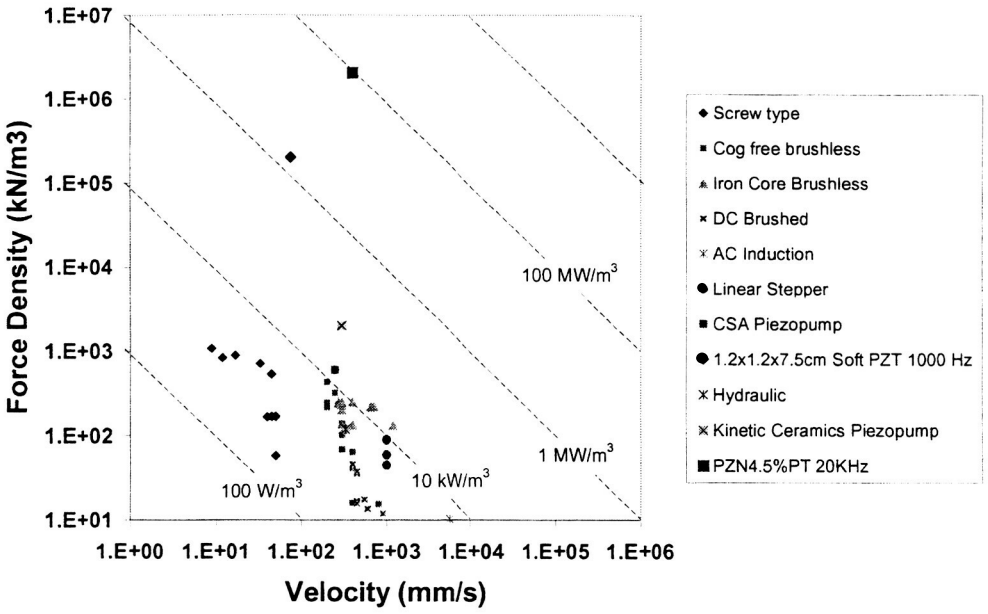

Figure 4. Force density vs. velocity for a range of available linear actuation systems. The diagonals are lines of constant power density.

2. Improved conventional piezohydraulic pump

The conventional piezohydraulic pump being developed consists of a piezoelectric stack actuator pushing a fluid through two check valves installed in a cylinder head. Increasing the drive frequency increases the flow rate. Recent focus has been on reducing the size and weight of the pump. This led to the identification of several design issues that had to be addressed.

One challenge with smaller pump sizes was the process of bleeding the air out of the system. The current system uses 3.175mm (1/8 in.) stainless steel tubing, which has an inner diameter of 1.75mm. The small size of the system components allows air to be easily trapped in the corners of machined parts and in the steel lines. A second challenge was associated with piston seals. The stacks were driving a piston that used o-rings to seal the fluid chamber. These o-rings were detrimental to the performance of the pump because they were difficult to seal the chamber, and they also compressed when the fluid was pressurized, creating losses in the system. To address these issues fluid cavities were designed to resist the entrapment of air, a static instead of a dynamic seal was used, and the pump geometry was adapted to use EPCOS cofired stacks.

2.1 Design Changes from Previous Generations

The major components of the redesigned piezohydraulic system consist of the pump assembly, a spool valve, high and low pressure accumulators, and a hydraulic actuator. A diagram of the fluid flow through the system components is shown in Figure 5. The low pressure accumulator is used to place a bias pressure on the fluid to prevent cavitation at high frequency. The high pressure accumulator allows the pump to build up a reserve of fluid pressure when the spool valve is in the locked position.

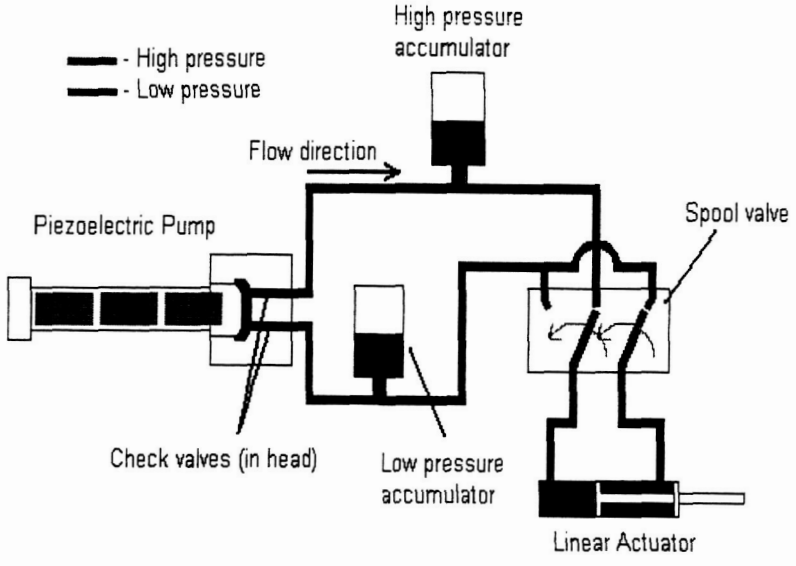

Figure 5: Fluid Flow Diagram

The spool valve was designed to replace the four way valve used on previous designs. It consists of six o-rings placed at the proper locations to allow pressurized fluid to flow to the hydraulic cylinder and actuate it. An illustration of the spool valve is shown in Figure 6.

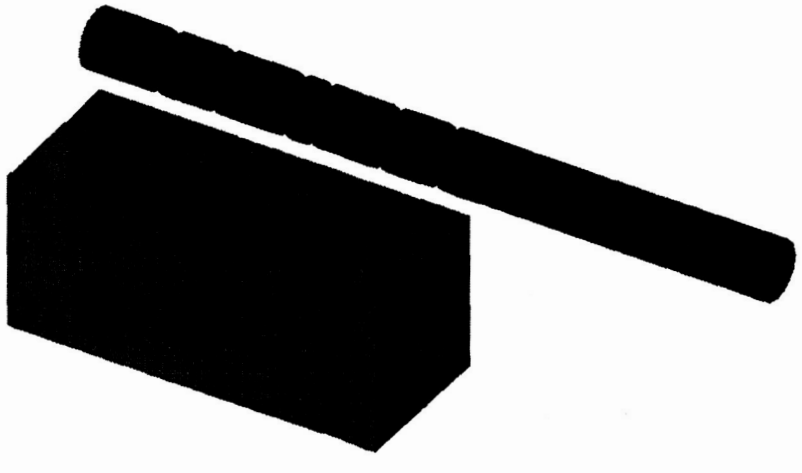

Figure 6: Spool Valve solid model

When switched, the pressurized fluid will switch inlets on the hydraulic cylinder and drive the actuator in the opposite direction while bleeding the low pressure fluid to the low side of the system. An important feature the spool valve has over the four way valve is the inclusion of a locked position. This middle position on the spool valve locks both the inlet and outlet of the hydraulic cylinder. This allows the user to lock the actuator in a desired position without having to use the pressure from the pump. This would be beneficial to allow the pump to recharge the high pressure accumulator when not in use. Figure 7 shows a picture of the spool valve.

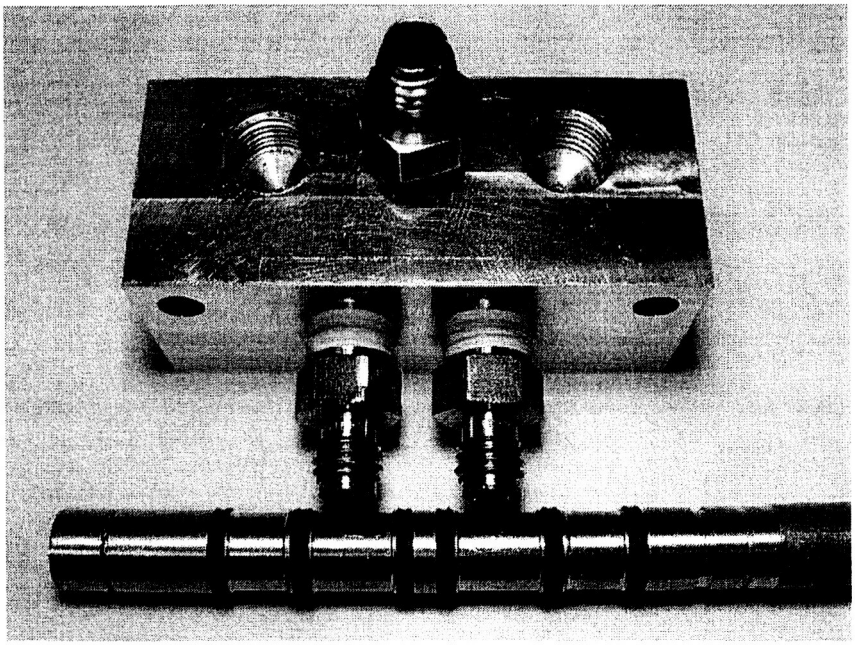

Figure 7: Spool valve photograph

The other design changes are directly related to the reciprocating pump component. The first and most obvious change to the pump is its material. The current pump was fabricated entirely of aluminum. This material was chosen over the previous steel due to its light weight and ease of machining. The overall size of the pump body decreased as a result of using the EPCOS PZT stack actuators. These actuators are cofired. In cofired actuators the layers of piezoceramic material are made much smaller than cut-and-bond stacks. This allows an actuator with smaller dimensions to be fully actuated with less voltage, reducing the complexity of the power supply that must be bundled with the pump when being used in an aerospace application. The EPCOS stacks consist of 5mm x 5mm layers of PZT potted in a rubberized plastic to protect the ceramic. Three 30mm long actuators are glued together end to end with Kapton and alumina ceramic insulating layers to form the driving component of the pump. Figure 8 shows the EPCOS driving actuator. The stacks are placed end to end to multiply the displacement of the end of the stack assembly

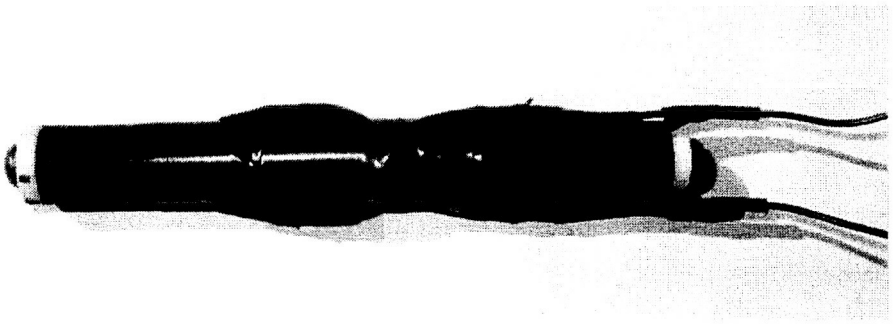

Figure 8: Three EPCOS stacks in shrink tubing

The drive system is placed inside a housing that consists of a housing tube, backing plate and screw cap. The PZT housing provides a solid foundation for the stacks to press against while allowing the wires to extend from the backing plate. Figure 9 shows the PZT housing. The left end of the housing screws into the cylinder head during operation. This allows the stack housing to be removed as a complete unit to protect the PZT from damage and allow quick reassembly.

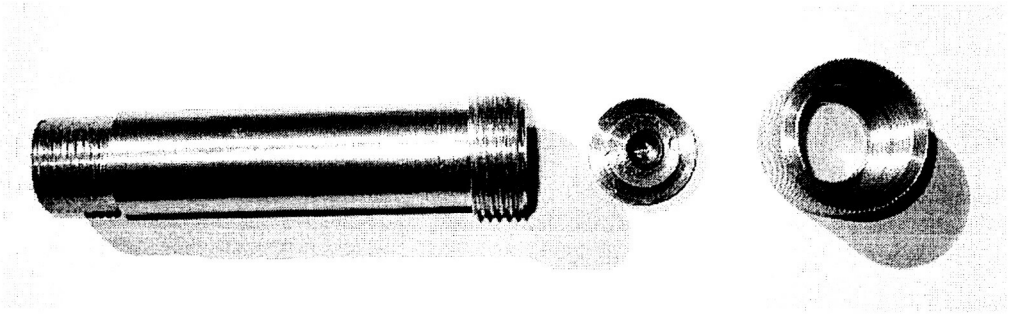

Figure 9: PZT housing

The cylinder head is the component that received the most changes over the previous system. The most important change deals with the separation of the fluid from the atmosphere. Previous designs actuated a piston and o-ring seal to pressurize the fluid. This design had difficulty sealing the fluid chamber, but more importantly, reduced the stiffness of the system through the compliance of the o-ring seal. The major design change in the redesign of this pump was to convert to a static sealing system instead of dynamic. This is performed by the use of a metal diaphragm to separate the fluid chamber from ambient pressures. The diaphragm is clamped between the two halves of the cylinder head using a cork gasket. The gasket is confined outside of the fluid chamber such that the gasket material is not in direct contact with the fluid. The diaphragm is stamped out of .008" stainless steel shim stock and cut to a diameter of 1.25". The diaphragm is stamped to a depth of .070".

To reduce compressibility effects, the diaphragm is placed in the fluid chamber with the stamped region recessed into the head. This orientation was possible because the head was machined to have a hemispherical fluid chamber. This was performed for two reasons: first to give the stamped diaphragm a recess for travel, second to aid in the bleeding of air from the system. With the small PZT induced displacements, any loss in stiffness of the system results in a significant decrease in system performance. The stacks end up doing work to compress the air bubble instead of moving the fluid. To this end, the cylinder head was designed with attention to simplifying the bleeding process. The bleed port was angled into the head so that the bleed hole is directly at the top of the hemispherical chamber. When oriented upright, all the air should collect at this point. Figure 10 shows a wireframe of the cylinder head which illustrates this feature. The inlet and outlet valves were placed close to the apex of the fluid chamber to aid in expelling air from the head.

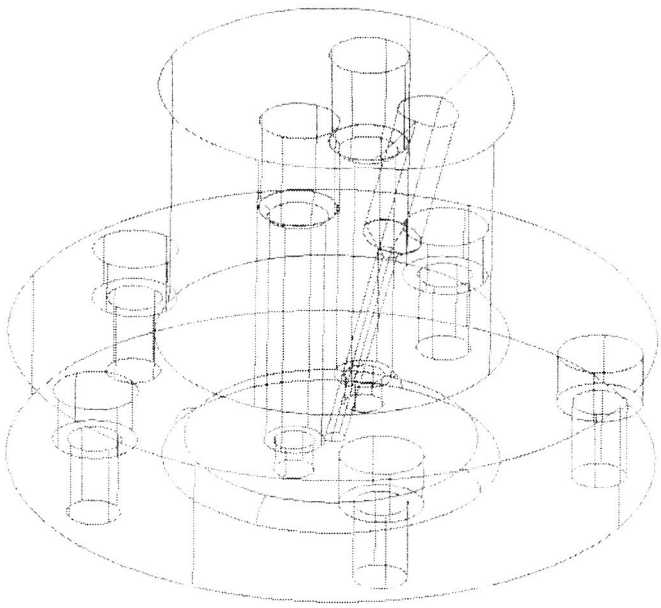

Figure 10: Wireframe of Top of Cylinder Head

2.2 System testing

Testing of the piezohydraulic pumping system was performed at the Georgia Tech Material Properties Research Laboratory. The amplifier driving the stack actuators is a Kepco (BHK 1000-0.2 MG) 0-1000V, 200mA amplifier. Assembly of the system consisted of screwing the PZT housing into the cylinder head until the stacks touched the diaphragm. Figure 11 shows a picture of the complete reciprocating pump.

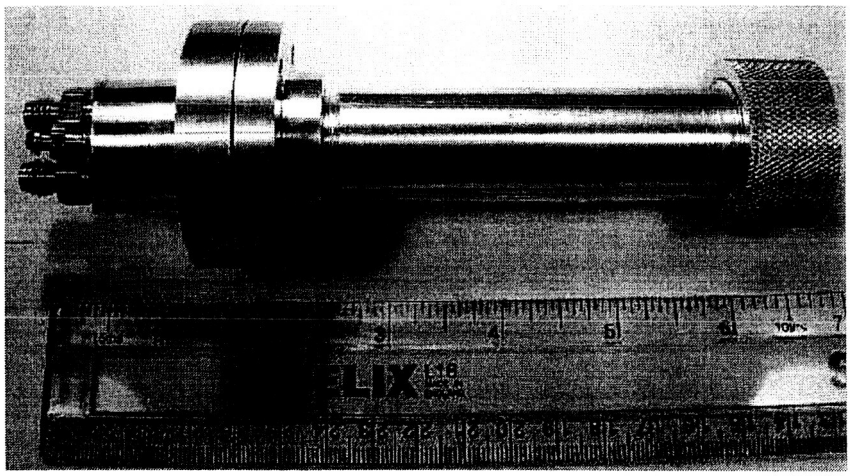

Figure 11: Assembled Pump Component

Bias pressure was then placed on the low pressure accumulator to preload the stacks and apply bias pressure to the fluid. A high pressure accumulator was not used in the experiments. For the first experiments, bias pressures of 125 psi and 160 psi were used. Pressure was measured using a gauge that was mounted inline with the high pressure side of the system. Figure 12 shows the experimental setup. The four-way valve was used in the experiments in place of the spool valve.

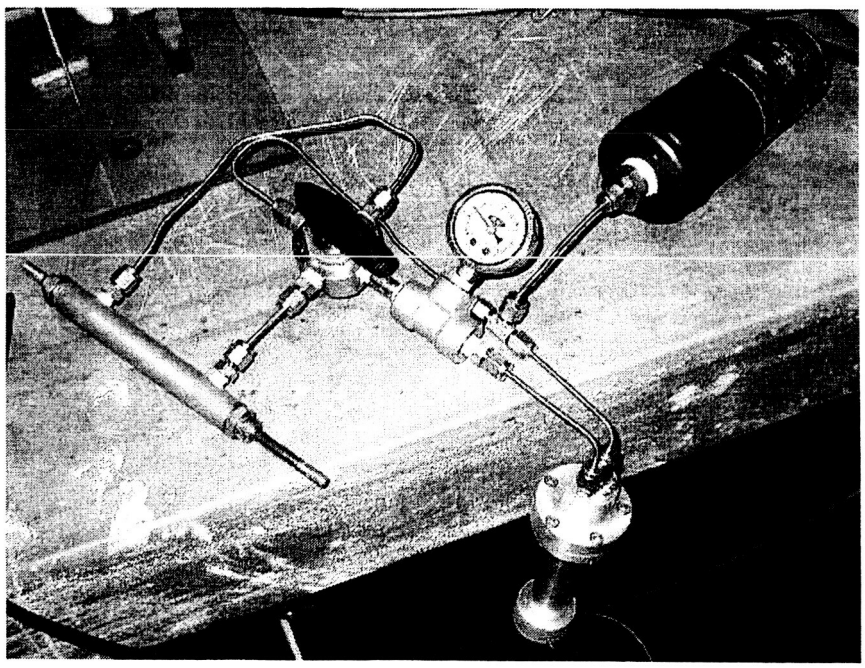

Figure 12: Experimental Setup of PZT Pump

The input voltage was set up and biased to apply a sine wave with a peak voltage of 150 V and a bias of 75 volts. The PZT was only be driven with positive voltages, hence the voltage offset. The pump was attached to a hydraulic cylinder with an effective piston area of 128.6 mm^2 (.1994 in^2) and bled of any air. Measurements of flow rate were taken using a stopwatch and a known fluid volume of the hydraulic cylinder. Flow rate measurements taken at various frequencies are plotted in Figure 13.

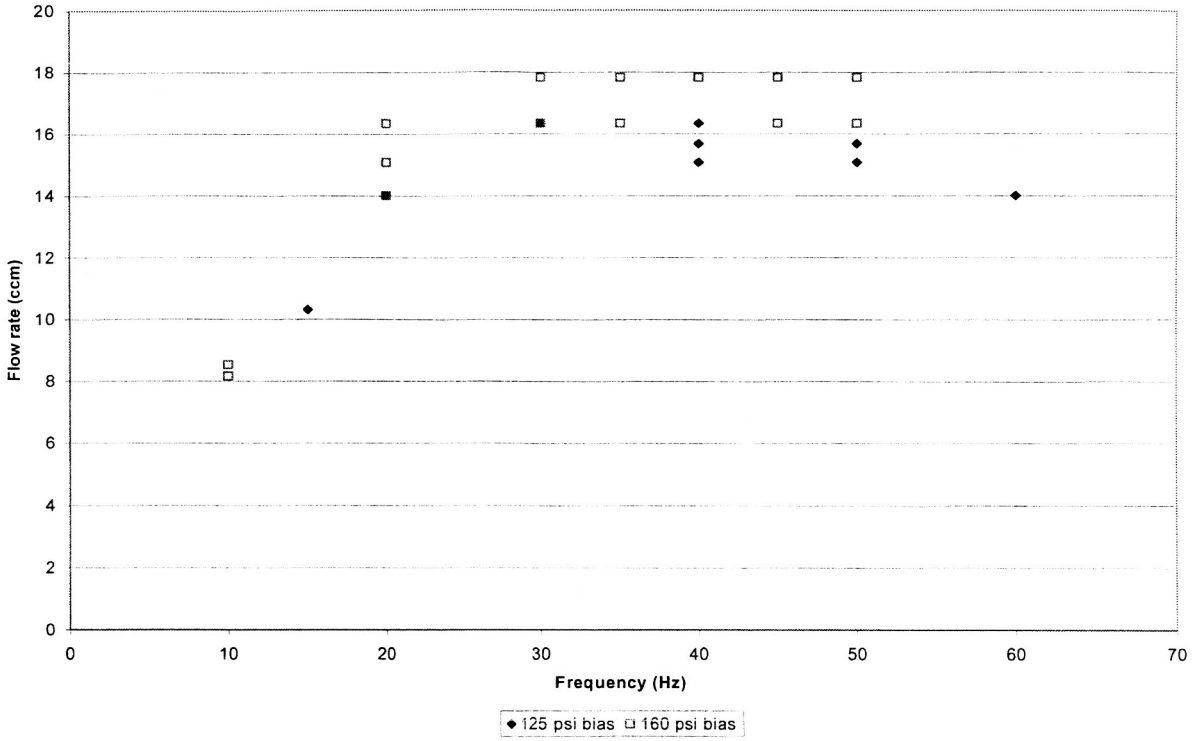

Figure 13: PZT Pump Flow rate vs. Frequency

The maximum flow rate obtained was approximately 18 ccm. This flow rate is lower than the previous generation pumps, however there are notable differences from the current model. The current generation has a maximum voltage input of 160V, much lower than the cut-and-bond driving actuators used in the past; the older actuators required a voltage of around 1000V to actuate. The lengths of the stacks are also much shorter than those used in previous generations. The EPCOS configuration consists of three 30mm stack actuators arranged end to end. The cut-and-bond actuators were as much as 300mm (12 in.) long. The pump bodies are also very different. The aluminum construction of the current pump is many times lighter than the stainless steel used in previous generations. Its small size contributes even more to its reduced weight. Utilizing the EPCOS stacks still provideed a pressure of 1.03 MPa (150 psi) over the bias pressure using only 150V. The light chassis weight and low voltage requirements allow these pumps to be used in parallel to provide necessary flow requirements. When coupled to a switching power supply, the power consumption will yield an efficiency that a traditional hydraulic system would never attain. With the

proper capacitive load power supply, even higher frequencies will be possible. Frequency is directly proportional to the output flow rate.

2.3 Designing with relaxor ferroelectric single crystals

At present, design with single crystals is not yet well understood. Many actuators have been produced and tested, but detailed material characterization data are still under development. Georgia Tech has been working with data collected by McLaughlin and Ewart at NUWC to help develop design criteria for reliable single crystal based actuators. Some of the results are included in Figure 14 (with their permission).

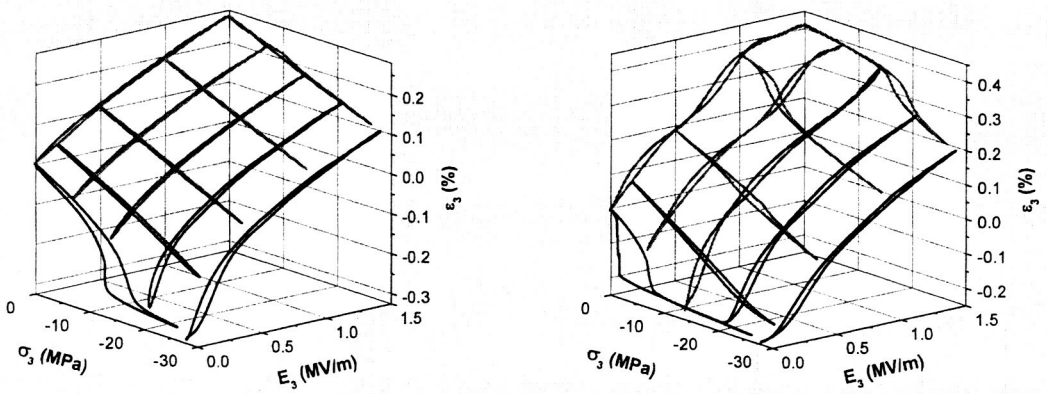

a) 20C b) 60C

Figure 14. Stress-Strain-Electric Field behavior or PMN-32%PT a) at 20C and b) at 60C

Single crystal actuators must be preloaded in compression to obtain reliable high cycle operation. Optimum operation is achieved in the upper planar region seen in Figure 14.a. This can be achieved with a 10 MPa bias stress, a 0.75 MV/m bias field, and a superimposed 0.5 MV/m oscillatory field. If the temperature is increased to 60C this material shows signs of multiple phase changes. Even though the hysteresis is small, it will lead to further heating. Although this composition could be used in the design and test phase, it is likely that a composition with less PT, e.g. PMN-28%PT would be a better candidate for the proposed actuators. This 28% PT material composition lies farther from the morphotropic boundary and will be more stable and show less hysteresis at 60C. Data of this nature are currently being developed and will be available for the design of reliable actuators in the coming months. Preliminary evidence suggests that driving the material through the phase changes to obtain more strain results in a short fatigue life. This is critical to understand for designing high frequency pumps.

2.4 Details of the reciprocating resonant pump under development

Existing Georgia Tech prototypes have produced pressure increases of 1200 PSI but at low flow rates. CHAP prototypes have produced similar pressure increases but with higher flow rates. As mentioned above, the proposed reciprocating resonant pump will use three high Q resonant systems to obtain large oscillations in fluid pressure that will be rectified into fluid flow using reed valves. The resonances are an LC oscillation in the drive circuit, a spring mass oscillation in the stack / head mass, and a tuned fluid oscillation in the output stage. The system is shown schematically in Figure 15.

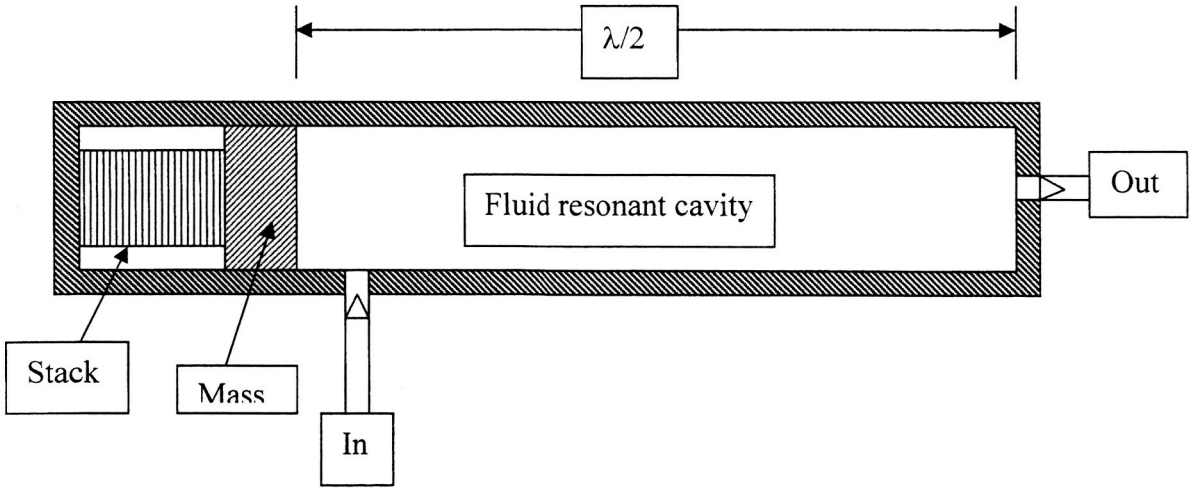

Figure 15. The proposed pump system will operate a resonating stack actuator with a head mass against a fluid resonant cavity. The cavity mode will be dependent on the end boundary conditions.

The proposed multi-resonant system is significantly differently from the technology developed under the CHAP program and the NASA funded Georgia Tech program. The external components are similar (small accumulator to provide a bias pressure and prevent cavitation, spool valve, actuator), but the pump has entirely new design characteristics.

2.4.1 Power requirements

The LC osillatory system will slew between 25 and 100 Watts between the inductor and the capacitor. The 20 KHz design frequency allows use of small off the shelf inductors (choke coils) matched to the capacitance of the stacks. This greatly simplifies the power supply design. Although this level of power is oscillating between the inductor and capacitor, not much is being dissipated. We anticipate developing a small 2 to 20 Watt power supply to drive the pumps. Note: 10W = 10 Nm/s will move 10N (about 2 lb) at 1 m/s. The large dielectric constant and low loss of the single crystals are critical to developing a high Q LC resonant power supply. A 1 microfarad capacitor (single crystal stack) with a 1 microhenry inductor will oscillate at 35 KHz. A 100 nF stack requires a larger inductor, but still relatively small. These

parameters are within our proposed design range and result in suitably small components. This will greatly simplify the power electronics relative to existing 10 cm scale piezopumps.

2.4.2 Stack oscillator

The spring-mass oscillation of the stack and head mass should produce a high Q resonance with large displacement. The Q of a similar system with soft PZT is much lower due to the lower coupling coefficient and higher loss tangent. The single crystal stacks are expensive. For this reason individual concepts and components are being tested using EPCOS cofired actuators.

A head mass/tail mass system was designed and constructed using three stacks for symmetry and frequency purposes. The three-stack resonator is the mechanical resonance side of a system that will have a fluid cavity excited using a similar arrangement. The system consists of a tail mass, head mass, three Epcos stacks, and a threaded prestress rod. A solid model of the resonator is shown in Figure 16. Three Epcos stacks were used in parallel to increase the stiffness of the system, which increases the required mass of the system to a manageable value. A 6-32 size threaded rod is used to apply a preload of 20MPa to the stacks. The threaded rod is five times the length of the stacks, or approximately 150mm. The larger length is necessary so that the spring constant of the bolt was low enough to not block the motion of the stacks, yet still provide necessary preload. The bolt also provides the necessary return force to avoid the stacks moving faster than the head mass.

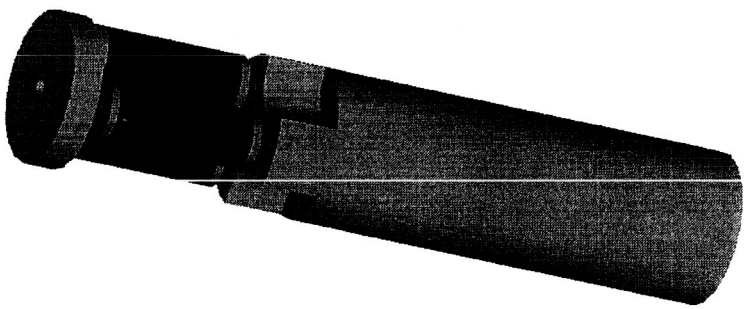

Figure 16: PZT Resonator Assembly

The resonator was designed to operate at approximately 20 KHz. The system is modeled as a spring mass system, with the preload bolt and PZT stacks as the springs. The spring constant of the PZT stack is calculated from known properties for PZT using Equation 1

$$k = \frac{AE}{L} \tag{1}$$

where A is the area of the piezoceramic ($4.5x10^{-5}$), E is the modulus (70 Gpa), and L is the length (30 mm); the spring constant for one PZT stack was determined to be 105 MN/m. The distributed mass of the stacks was neglected.

Knowing the spring constant available, a head mass was determined using Equation 2. In this equation, k_T is the total spring constant, which is the sum of the three PZT stack spring constants and the preload spring constant. A three stack arrangement was chosen because three stacks in parallel operating at 20 kHz requires a head mass of approximately 20g.

$$m = \frac{k_T}{(2\pi f)^2} \tag{2}$$

The configuration of the stacks and the selection of the preload bolt were determined iteratively. The system requirements are quite complex, but can be narrowed down to three main requirements. First, the PZT stack must be placed under an initial compressive stress of around 20 MPa, hence the use of a preload bolt. Second, the stack is capable of a 1000 microstrain deflection, therefore the preload mechanism must stretch $3x10^{-5}$m after being preloaded without significantly increasing the stress on the PZT; an increase of 5 MPa is considered acceptable. This requirement translates to a preload mechanism with a low stiffness. The final requirement is that the preload mechanism must be able to supply the return force necessary to pull the head mass back after it has reached its full displacement. This force was calculated by determining the peak acceleration of the mass, Equations 3 and 4,

$$x = \delta \sin(\omega t) \tag{3}$$

$$\left\| \frac{d^2 x}{dx^2} \right\| = \delta (2\pi f)^2 \tag{4}$$

where, δ is the peak displacement and f is the desired frequency, in Hertz. The necessary return force was then calculated by multiplying the peak acceleration by the head mass. The preload system must be able to provide the necessary return force because the PZT stacks are not rigidly attached to the head mass. This was done because the stacks may not be placed in tension. Therefore the bolts must be able to carry the return load to avoid "floating" the head mass at high frequency.

A single bolt made of 18-8 stainless steel size 6-32 was chosen as the preload mechanism. The length of the threaded rod was made five times the length (150 mm) of the PZT stack actuator; this allows for a lower spring stiffness, while still providing the necessary return force at maximum deflection. The spring

stiffness of the preload rod was calculated using Equation 1, where A is the 6-32 effective tensile area and E is the modulus of steel. Figure 17 shows the completed PZT resonator.

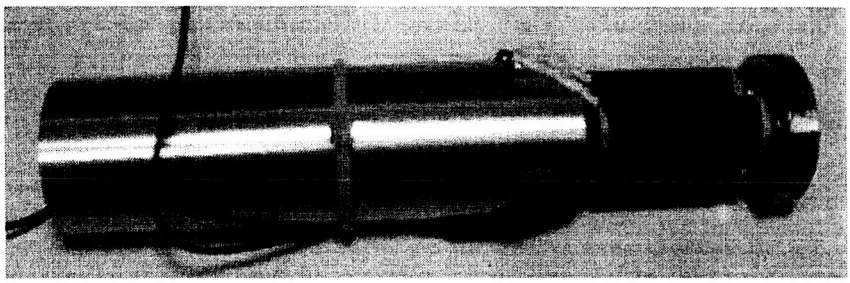

Figure 17: Three Stack PZT Resonator

Testing of the three stack PZT resonator was performed using a Protec laser Vibrometer and data acquisition system. The experimental setup is shown in Figure 18. Notice the resonator set up on a microphone stand in the lower right corner and the laser vibrometer to the left in Figure 18. The laser vibrometer uses a laser pointed at the head mass to measure the vibration of the head in order to characterize the frequency response of the resonator. The data from the vibrometer passes through signal conditioners and is input to a software package that allows the user to view the information in different bases and time scales.

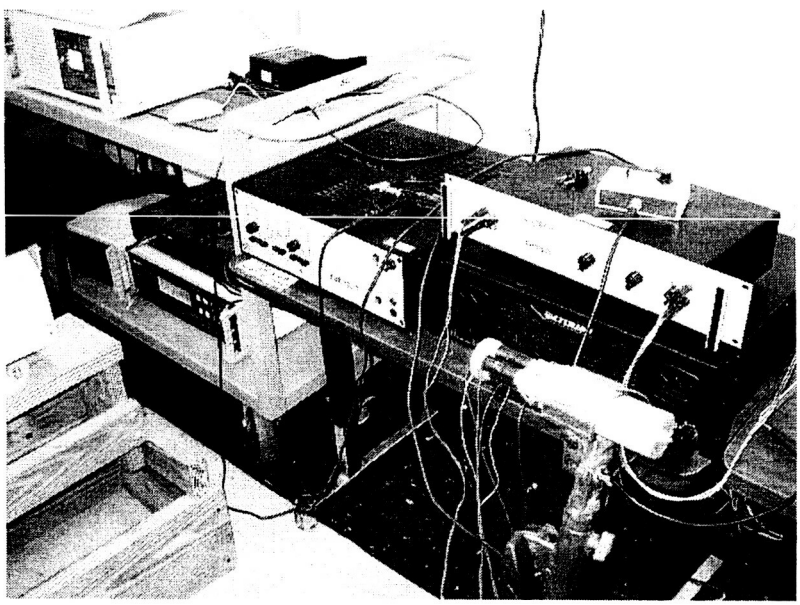

Figure 18: Experimental Setup of Laser Vibrometer

A voltage reference input was connected to the data acquisition system from the output of the amplifier used to drive the PZT actuators. This would normalize the vibration data and account for any fluctuation in driving voltage and not skew the vibration results. A power amplifier was used to drive the stacks using the

function generator in the vibrometer package. A 1V peak to peak sine wave was used to drive the resonator. Low voltages may be used because the resonant frequencies are not dependent on the level of excitation. A frequency sweep from 1-30kHz was performed, and the maximum velocities were monitored. The resonant frequency of the resonator system was narrowed down to around 10kHz; this result is much less than the 20kHz desired frequency. Figure 19 shows a graph of the magnitude of velocities around the 10 kHz range. The lower than calculated resonant frequency was expected due to the design calculations neglecting the mass of the actuators and preload rod. The order of magnitude increase in velocity at resonance will be utilized to improve pump performance.

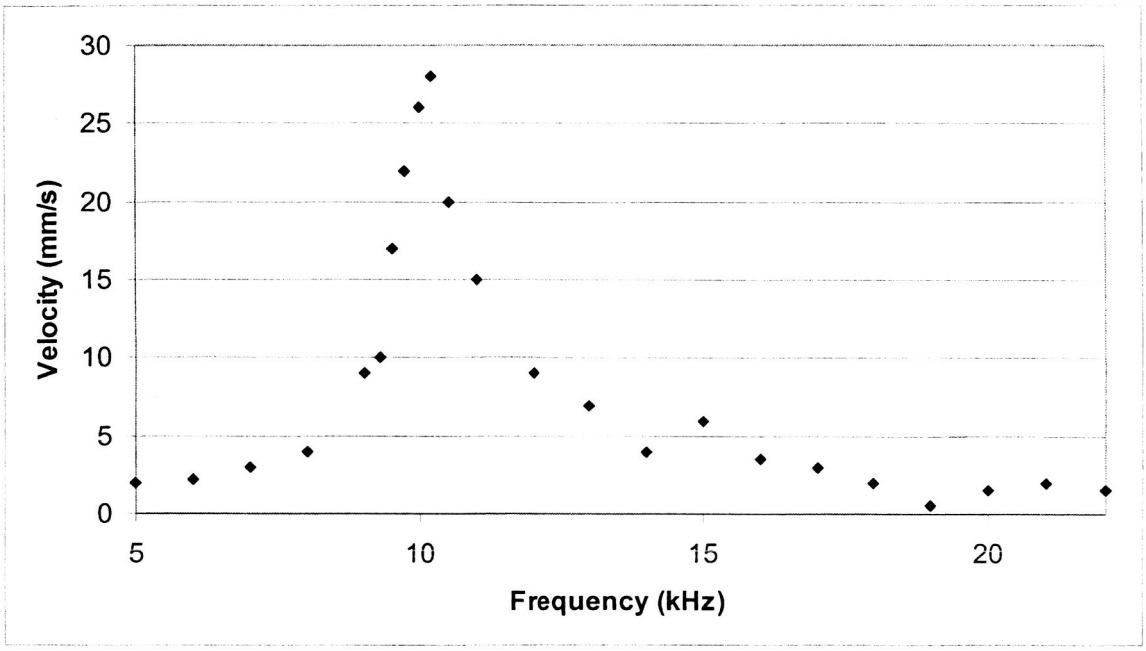

Figure 19: Velocity Magnitude at First Natural Frequency

2.4.3 Fluid resonant cavity

The fluid will be driven into resonance in a quarter wave or half wave mode depending on the end constraint boundary conditions. Tube wall thicknesses will affect the propagation velocity in the fluid. Hydraulic resonant cavities have been designed with very high Q. Our system will be designed with consideration of non-linear effects and bulk viscosity. The high Q of the resonant fluid cavity will result in a large pressure amplification. Bleed holes will allow a small amount of fluid to be extracted from the cavity on the high pressure excursion through the outlet port and to enter on the low pressure excursion through the inlet port. The ports will be small relative to the tube size to allow high Q oscillation. A 20 KHz resonant cavity filled with water will have dimensions on the order of 10 mm diameter and 40 to 80 mm length.

The initial design and construction of the fluid resonant cavity is to obtain gain and frequency measurements. A resonator has been designed and constructed. Testing is just commencing.

The design of the fluid resonator was centered around a target resonant frequency of 20 kHz. The cavity is cylindrical, with one flat end capable of being vibrated while the other end is rigid to promote wave reflection. The vibrating end will set up a pressure wave that will propagate through the fluid at the speed of sound. The light oil that will be used has properties similar to water, therefore a sound speed of 1500 m/s was used in the calculations. The desired frequency of 20kHz corresponds to a period of 50μs. Therefore in this period of time the wave must travel from one end of the cavity to the other and back again. Equation 5 shows the calculation of the fluid cavity length, *L*.

$$2L = 1500m/s \cdot 50\mu s \tag{5}$$

This equation yields a cavity length of 37.5mm. This size will produce a very compact resonator. Figure 20 shows a wireframe model of the resonator fluid cavity.

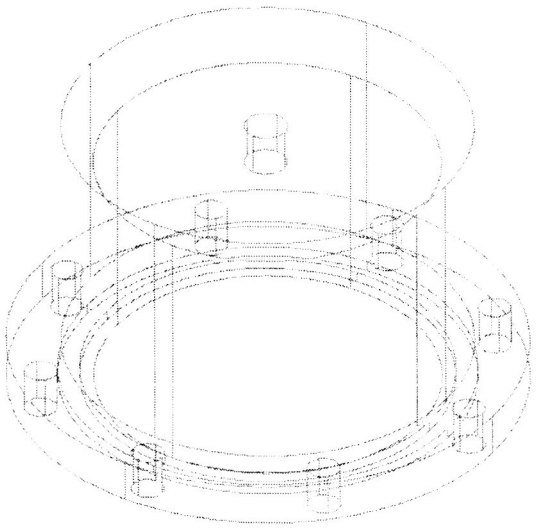

Figure 20: Resonating Fluid Cavity

The displacement function of the ends of the PZT stack actuators must be investigated to determine the peak velocity of the vibrating wall. This is performed using the maximum displacement of the stack actuators. The stacks have a free displacement of 1000 microstrain, which for a 30mm stack corresponds to a displacement of .03mm. Therefore, the position function of the end of the actuator is of the form $x=D\sin(\omega t)$, where D is half the maximum free displacement. The peak velocity is then the derivative of position or $v=D\omega\cos(\omega t)$. If ω is the frequency, in radians, then the peak velocity of the end of the stack actuators is 1.88m/s. This velocity is subsonic when compared to the speed of sound in the fluid. This result is favorable because the compressibility of the fluid need not be taken into account.

The fluid side of the resonator system is sealed from the atmosphere using an aluminum diaphragm. Aluminum was chosen because of its low stiffness. The chosen thickness of the diaphragm must be a balance between a flexible vibrating wall and a rigid wave reflecting surface. Figure 21 shows an exploded view of the two halves of the resonator along with the diaphragm and o-ring.

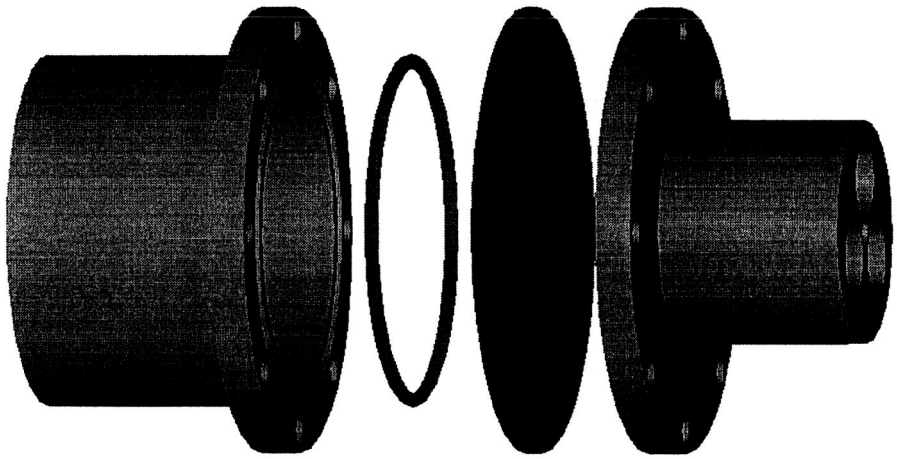

Figure 21: Fluid Resonator Assembly

Different thickness diaphragms are manufactured to test the effect of diaphragm thickness on system response. Three PZT stack actuators are oriented symmetrically around the surface of the diaphragm to promote uniform vibration. The concerns with diaphragm stiffness will not be met during this concept stage, but will have to be met when the system is converted to a pump. These concerns deal with the diaphragm's ability to remain in constant contact with the ends of the stack actuators. The diaphragm must be stiff enough to avoid separation of the stacks from the diaphragm at the 20 kHz operation frequency. Separation of these components could result in failure of the stack actuator. In this concept stage, the displacement of the actuators will be minimal, because the cavity will be filled with liquid and there are no inlets or outlets. The stacks will be pushing against a solid column of water. When the system is adapted to use in a pump application, there will be exits for the fluid, which will result in a higher displacement of the stack actuators. The diaphragm's ability to remain in contact with the stack actuators will have to be assessed at that time.

The testing of the fluid resonator system is still in progress. The stack actuators will be driven by a power supply capable of producing the necessary 150V at the selected frequency. Figures 22 and 23 show the completed resonator assembly.

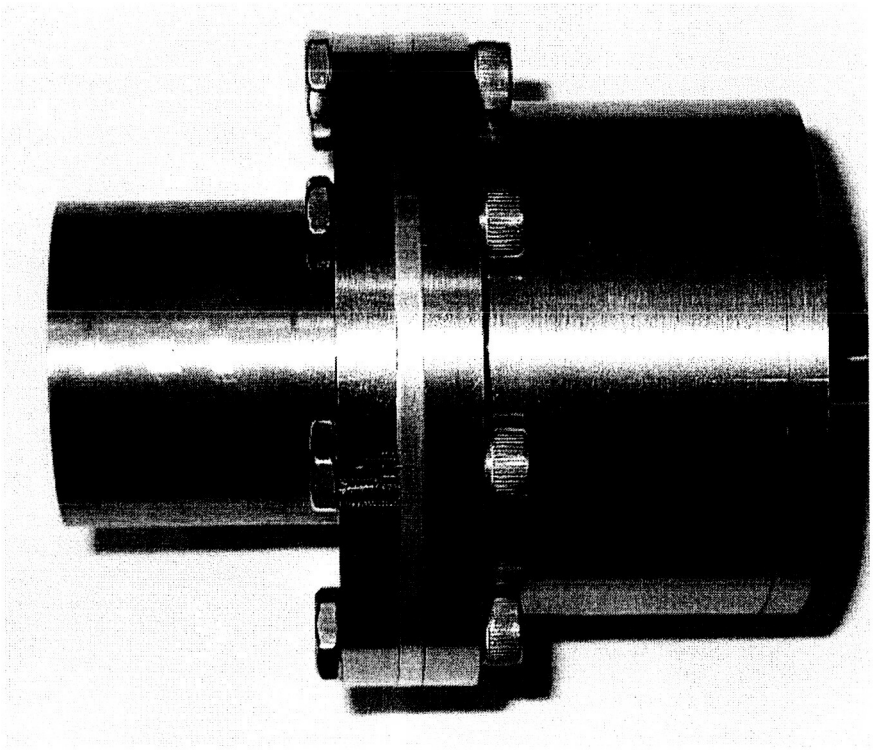

Figure 22: Resonator Assembly (side view)

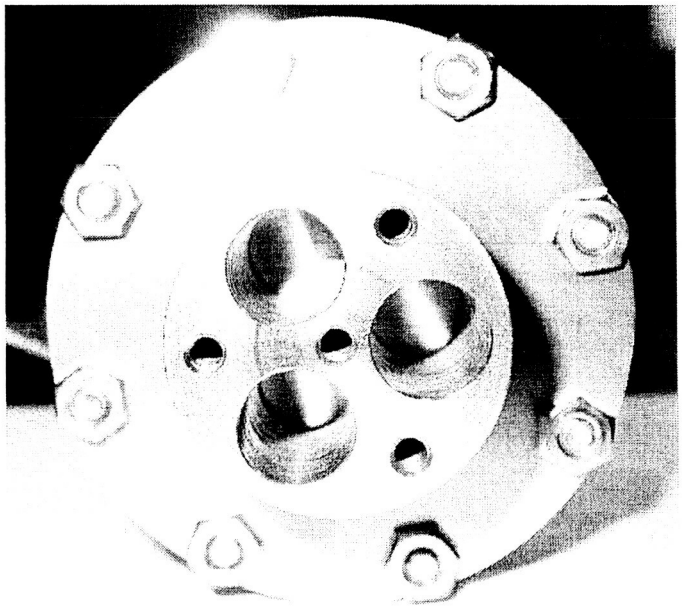

Figure 23: Resonator Assembly (end view)

Pressure in the fluid will be measured using a fast response pressure sensor capable of measuring pressure transients with a rise time of 1 microsecond or more. Once the fluid cavity is filled and all the air removed, the piezoelectric actuators will be driven with a frequency sweep to find the frequency of the driving

system that produces resonance in the fluid. From this data, the peak pressure in the fluid will be measured, and methods to use this pressure to power a hydraulic cylinder will be devised.

2.4.4 Valves

Fluid will be fed into and drawn out of the resonant tube through reed valves or through fluidic diodes. Rough calculations show that reed valves are at the limit of operation at 20 KHz if they depend solely on their stiffness for a return force. A type of micro poppet valve has been conceptually designed and may be developed that is very low mass and uses a small amount of back flow to draw them closed. Preliminary analysis of the dynamics indicates that a 50 KHz valve can be constructed. The poppet will move 100 microns, have a 1.2mm diameter and move 200 microns under a pressure differential of 280 KPa (40 PSI) This will open a 1mm tube during the high pressure portion of the resonant cycle. Several different high frequency check valve concepts have been considered including reed valves and several variations of micro-machined valves.

Reed valves are known for high frequency response and ability to seal high pressures such as combustion pressures in a two stroke combustion engine. In order to take full advantage of the frequency characteristics of the PZT material, the investigation into reed valves will look at driving frequencies of 10kHz to 20kHz. In order to operate a pumping system in the tens of kilohertz, the reed valves must have a natural frequency in the same range, preferably higher than the maximum operating frequency. For the natural frequency calculations, spring steel thicknesses of .254mm (0.010in.), .381mm (0.015in.), and .508mm (0.020in.) were used. The valve was assumed to be a cantilevered beam fixed at one end. The natural frequency of the beam with its mass distributed along its length is given by Equation 6,

$$\omega_n^{\ 2} = (3.52)^2 \left(\frac{EI}{ml^3} \right) \tag{6}$$

where I is the second moment of inertia in the form of Equation 2.

$$I = \frac{bt^3}{12} \tag{7}$$

In these equations, b is the width of the beam, l is the length, and t is the thickness. The calculations were performed for two natural frequencies, 10kHz and 20kHz. Using the given thicknesses and a common width of 5 mm, Equation 1 was solved for the length of the beam. Table 1 shows the results of these calculations.

Table 1: Natural Frequency Calculations for 10kHz and 20kHz

Natural Frequency (Hz)	Thickness (mm)	Maximum Length (mm)
10000	.254	4.60
10000	.381	5.63
10000	.508	6.50
20000	.254	3.25
20000	.381	3.98
20000	.508	4.60

All the necessary lengths required for the desired natural frequencies are manageable. There would be enough exposed valve to cover the inlet and outlet holes and still perform their function. The only questionable valve length is the .254 mm thickness operating at 20kHz. A length of 3.25mm does not leave much room for a fluid passage underneath. The inlet and outlet holes need to be of sufficient size as not to choke the system with excessive fluid resistance.

A more in depth look into the operation of the reed valves suggests that fatigue issues will have a very strong influence on their design. Because of their high operating frequency, the valves must be designed for infinite life. In order to have infinite life, the maximum alternating stress must be low enough, as defined by one of the standard fatigue criterion. This alternating stress value is directly affected by how far the reed valve bends in operation. The fatigue calculations begin with the determination of the endurance limit. According to Norton, the uncorrected endurance limit for steels with an ultimate tensile strength of less than 200ksi is one half the ultimate tensile strength. For the calculations in this paper, 1095 carbon steel quenched and tempered at 200 °F will be used. Table 2 illustrates some of the properties of this material.

Table 2: Properties of 1095 Carbon Steel Q&T at 200 °F

Density (kg/m^3)	7800
Modulus (Pa)	$207x10^9$
Yield Strength (Pa)	$552x10^6$
Ultimate Tensile Strength (Pa)	$896x10^6$

Using the value of the ultimate tensile strength, the uncorrected endurance limit is 448 MPa. Now that this value is known, a series of correction factors may be calculated to account for size, surface, and other conditions during the loading cycle. Equation 8 shows the correction factors according to Norton.

$$S_e = C_{load} C_{size} C_{surf} C_{temp} C_{reliab} S_e' \tag{8}$$

Because the valves are in a bending mode, C_{load} equals 1; similarly, C_{size} equals 1 due to the small size of the valves. For the surface effect correction factor, we will assume the valve material has a ground finish. Therefore, the correction factor is calculated in Equation 9.

$$C_{surf} = 1.58(S_{ut})^{-0.085} \tag{9}$$

This calculation results in a surface correction factor of 0.89. The temperature effects are negligible, therefore C_{temp} equals 1. For reliability, a 99.9% value is desired, which results in a correction factor of 0.753. These correction factors are combined to produce a corrected endurance limit of 299 MPa. This value may then be input into the desired failure criterion to determine the maximum allowable load.

The failure criterion used is the modified Goodman criterion. This criterion relates the mean and alternating stresses to experimental evidence of failure. Equation 10 illustrates the failure line of the modified Goodman criterion.

$$\sigma_a = S_e \left(1 - \frac{\sigma_m}{S_{ut}} \right) \tag{10}$$

In this equation σ_a and σ_m are the alternating and mean stresses, respectively; S_e is the corrected endurance limit, and S_{ut} is the ultimate tensile strength. In the case of the reed valves, the mean stress is equal to the alternating stress, resulting in Equation 11.

$$\sigma_a = \frac{S_e}{\left(1 + \frac{S_e}{S_{ut}} \right)} \tag{11}$$

With this equation, a maximum possible alternating stress is calculated as 224 MPa. Therefore, the maximum stress experienced by the reed valve is the mean stress plus the alternating stress, in this case $2 \cdot \sigma_a = 448 MPa$. This is the maximum stress that may be experienced by the reed valves and still maintain infinite life. The deflection of the reeds are then calculated using Equations 12 through 14. Equation 12 is the deflection of a beam under applied force.

$$y_{max} = \frac{FL^3}{3EI} \tag{12}$$

Equation 13 is the maximum stress on a beam due to a force applied

$$\sigma_{max} = \frac{FLt}{2I} \tag{13}$$

Solving Equations 12 and 13 for *FL/I* and combining results in Equation 14

$$y_{max} = \frac{2l^2\sigma}{3tE} \tag{14}$$

In Equation 14 the stress is the maximum stress the beam can take and retain infinite fatigue life. Using Equation 14 to calculate the tip deflection, it was noticed that the l^2/t terms were the same for each thickness and length for a given resonant frequency. Therefore the maximum tip displacement was only a function of frequency. The maximum tip displacement to maintain infinite fatigue life for the 10kHz and 20 kHz valves is .1204mm and .0602mm, respectively. The reed valve tip displacement can be limited by putting a stop behind it.

The results of this investigation into the use of high speed reed valves to operate a reciprocating pump were interesting. Making a beam vibrate at frequencies in the tens of kilohertz makes fatigue a dominating factor in its operating life. Infinite fatigue life is necessary to have a useful part in these conditions, and this constraint limits the amount of stress that can be placed on the material. The tip displacement of .1204mm for 10kHz mediocre at best, but the .0602mm displacement for 20kHz is unacceptable. Such a small displacement would put an incredible amount of fluid resistance in the system. The problem with the cantilevered beam reed valve is the fatigue life. If the valve could be modified to operate on a hinge, the stresses on the valve material would be minimal, satisfying the fatigue constraint. The tradeoff is the valve would no longer have a return force. The flow of the system would have to be routed around the reed flap to promote the opening and closing of the valve.

3. Planned work

The planned work for the third year of the project includes completion of the testing of the fluid cavity, design and testing of a tuned electro-mechanico-fluidic resonant system, and design and development of an LC resonant drive system. This should result in a highly compact, light weight, high specific power and power density actuation system.